2021 61st IEEE Conference on Decision and Control (CDC)
December 6-9, 2022. Cancún, Mexico

Using local reachability sets in guiding mobile actuator and its orbiting sensors to approximate state feedback kernels in output control of PDEs

Michael A. Demetriou

Abstract— **This paper considers a class of distributed parameter systems that can be controlled by an actuator onboard a mobile platform. In order to avoid computational costs and control architecture complexity associated with a joint optimization of actuator guidance and control law, a suboptimal policy is proposed that significantly reduces the computational costs. By utilizing a continuous-discrete optimal control design, a mobile actuator moves to a new position at the beginning of a new time interval and resides for a prescribed time. Using the cost to go with variable lower limit, the optimization simplifies to solving algebraic Riccati equations instead of differential Riccati equations. Adding a hardware feature whereby the mobile sensors are constrained to stay within the proximity of the mobile actuator, a feedback kernel decomposition scheme is proposed to approximate a full state feedback controller by the weighted sum of sensor measurements.**

I. Introduction

This paper continues earlier efforts to minimize the computational costs and reduce the controller architecture complexity associated with the use of mobile actuators in the control of PDEs. Formulated as a joint control-plus-guidance problem, the resulting solution requires both the costate and the guidance to be integrated backwards in time. To avoid this, a suboptimal controller was proposed in [1], [2]. The basic idea is to use a suboptimal policy wherein the lower limit of the cost to go performance index was used at the beginning of a new time interval to select the next actuator position. This required the solution to algebraic Riccati equations as opposed to differential Riccati equations. Incorporating the constraints of the platform dynamics which prohibited the platform to traverse large distances in infinitely small time intervals, the selection of the actuator location was restricted to the locations in the spatial domain that would guarantee approximately controllability of the resulting operator pair (state and input operator) *and* respect the motion constraints of the mobile platform. This gave rise to reachability sets that were time-varying and dependent on the current actuator position.

While the optimal control with the actuator motion provided significant computational savings and reduced controller complexity, it required access to full state. To remove this requirement a collocated actuator-sensor was proposed [2] but it did not utilize any optimality for controller performance. Instead the decision to move the actuator to a new location was based on stability arguments. An alternative to this is to build a state estimator using either mobile sensors onboard different platforms, or use fixed-in-space sensors. Such a configuration will certainly improve the compensator performance but it will increase the computational cost by requiring the real-time implementation of a state observer and heavier communication costs between the sensors and the actuator-plus-control unit.

To avoid the implementation of a state observer, this paper proposes to use a network of sensors hovering the actuator that are used to approximate a dynamic full-state controller by a static output feedback controller. This is achieved by using computational geometry to decompose the associated with the feedback operator used in the controller description and replace the full-state feedback by a weighted sum of sensor measurements. This kernel decomposition is based on a modification of Centroidal Voronoi Tessellations (CVT) heavily utilized in [3], [4], [5], [6] to approximate the feedback kernel by pointwise sensor. The modification proposed in [7], [8], [9] decomposed the spatial domain into cells that had the same area under the feedback kernel. Subsequently it computed the corresponding feedback gains and implemented this approximated state feedback.

The above two are combined and constitute the contribution of this work.

1) Present a guidance scheme using time-varying reachability sets to reposition the actuator platform at the beginning of a time interval.
2) Propose a feedback kernel decomposition scheme to compute time-varying sensor positions and their associated gains to approximate a full-state feedback controller by the weighted sum of sensor measurements.
3) Extend the results of the modified CVT method to restrict the sensors in the vicinity of the actuator position by coinciding the vicinity region by the time-varying reachability set, thereby ensuring that the mobile sensors are always orbiting the actuator position.
4) Demonstrate to 1D and 2D advection-diffusion PDES.

II. Problem formulation

The emphasis of the proposed work is on spatially distributed processes in one and two spatial dimensions. Partial differential equations in 1D and 2D can be viewed as evolution equations Hilbert space $\mathcal{X}$ and given by

$$\dot{x}(t) = \mathcal{A}x(t) + \mathcal{B}u(t), \quad x(0) = x_0 \in \mathrm{dom}(\mathcal{A}). \qquad (1)$$

The process state operator in (1) $\mathcal{A} \in L(\mathcal{V}, \mathcal{V}^*)$ and the control input operator $\mathcal{B} \in L(\mathcal{U}, \mathcal{V}^*)$. The use of the additional spaces $\mathcal{V}, \mathcal{V}^*$ allow for unbounded operators often representing spatial differentiation in the expression for the

M. A. Demetriou is with WPI, Aerospace Engineering Department, Worcester, MA 01609, USA, mdemetri@wpi.edu. The author acknowledges financial support from NSF-CMMI grant # 1825546.

state operator. The state space $\mathcal{X}$ is a Hilbert space and the two interpolating spaces are the reflexive Banach space $\mathcal{V}$ that is continuously and densely embedded in $\mathcal{X}$ and its conjugate dual $\mathcal{V}^*$. Following [10], we have $\mathcal{V} \hookrightarrow \mathcal{X} \hookrightarrow \mathcal{V}^*$ with both embeddings dense and continuous. This Gelfand triple also allows one to define the input and output operators in different spaces. In the definition of the input operator, the control space $\mathcal{U}$ is a finite dimensional Euclidean space.

Examples of PDEs that can be represented by (1) are the 1D and 2D advection-diffusion PDEs. The 1D PDE is

$$\begin{aligned}\frac{\partial x}{\partial t}(t,\xi) = \alpha\frac{\partial x^2}{\partial \xi^2}(t,\xi) - \beta\frac{\partial x}{\partial \xi}(t,\xi) \\ -\gamma x(t,\xi) + b(t,\xi)u(t),\end{aligned} \tag{2}$$

with Dirichlet boundary conditions $x(t,0) = 0 = x(t,\ell)$ and initial condition $x(0,\xi) = x_0(\xi)$. The function $b(t,\xi)$ is the spatial distribution of the actuating device and is explicitly made time-dependent to reflect the time-varying nature of the actuator position in the spatial domain $\Omega = [0,\ell]$. When the actuator spatial distribution represents a pointwise-in-space distribution, then the control term is given in weak form by

$$\langle bu, \phi(\xi)\rangle = \int_0^\ell \delta(\xi - \xi_a(t))u(t)\phi(\xi)\,\mathrm{d}\xi = \phi(\xi_a(t))u(t), \tag{3}$$

where $\xi_a(t)$ denotes the time-varying centroid of the actuating device and $\phi \in H_0^1(0,\ell)$ is the test function.

Similarly, a typical PDE on a 2D spatial domain that can be represented by (1), is given by

$$\begin{aligned}\partial_t x(t,\xi,\psi) &= \alpha\Delta x(t,\xi,\psi) - \beta(\xi)\cdot\nabla x(t,\xi,\psi) \\ &\quad -\gamma(\xi,\psi)x(t,\xi,\psi) + b(t,\xi,\psi)u(t),\end{aligned} \tag{4}$$

in $\Omega \times (0,\infty)$ with Dirichlet boundary conditions $x(t,\xi,\psi) = 0$ on $\partial\Omega \times (0,\infty)$ and initial condition $x(0,\xi,\psi) = x_0(\xi,\psi)$. When the actuator is mobile with centroid $(\xi_a(t),\psi_a(t))$ and has a spatial distribution given by the Dirac delta function, the control term is given by

$$\begin{aligned}\langle bu, \phi\rangle &= \iint_\Omega \delta(\xi - \xi_a(t))\delta(\psi - \psi_a(t))u(t)\phi(\xi,\psi)\,\mathrm{d}\psi\mathrm{d}\xi \\ &= \phi(\xi_a(t),\psi_a(t))u(t),\end{aligned} \tag{5}$$

In the ideal case of full-state availability, one can design a state feedback controller for (2) and (4) to satisfy performance requirements often described by a performance index. A widely used index is the one associated with the linear quadratic regulator and the resulting full-state feedback controller signal has the form

$$u(t) = -\mathcal{K}(t)x(t). \tag{6}$$

The feedback operator $\mathcal{K}(t)$ may or may not be time-varying. When a time-varying input operator $\mathcal{B}(t)$ is assumed, as the one associated with (3) or (5), or when the LQR performance index is given by a finite horizon linear quadratic functional

$$\begin{aligned}J &= \int_0^T \langle x(\tau), Qx(\tau)\rangle_X + u^T(\tau)R^{-1}u(\tau)\,\mathrm{d}\tau \\ &\quad +\langle x(T), \mathcal{M}x(T)\rangle,\end{aligned} \tag{7}$$

the feedback operator will be time-varying. The operators $Q, R, \mathcal{M}$, defined in the respective spaces are assumed coercive operators. The particular case of a time-varying input operator arises when the actuator device is continuously repositioned within Ω, see (3) or (5).

While the problem of joint optimal control and actuator motion has been summarized in [2] and as the dual problem of the optimal filtering with mobile sensor established in [11], [12], [13], this work will handle the actuator guidance problem separately from the derivation of the optimal controller. For a prescribed actuator guidance, resulting in a given input operator $\mathcal{B}(t)$, one would need to find the optimal controller corresponding to the associated operator $\mathcal{B}(t)$. Thus, the optimal control problem with a prescribed actuator guidance becomes a suboptimal controller of the joint actuator-plus-controller optimization problem. However, the optimality comes in the form of real-time implementability.

For a given time-varying $\mathcal{B}(t)$ associated with (3) or (5), one must solve the Operator Differential Riccati Equation

$$-\dot{\mathcal{P}} = \mathcal{A}^*\mathcal{P} + \mathcal{P}\mathcal{A} - \mathcal{P}\mathcal{B}(t)R^{-1}\mathcal{B}^*(t)\mathcal{P} + Q = 0, \tag{8}$$

in order to obtain the corresponding the time-varying feedback gain operator $\mathcal{K}(t) : \mathcal{V} \to \mathcal{U}$. The terminal condition for (4) is $\mathcal{P}(T) = \mathcal{M}$, and upon successful solution to (4) via backwards-in-time integration, one obtains the feedback operator in terms of the solution $\mathcal{P}(t)$ as $\mathcal{K}(t) = R^{-1}\mathcal{B}^*(t)\mathcal{P}(t)$.

To realize (6) using (8), one must also generate in real-time the state estimate of the process state $x(t)$. An alternate to state reconstruction, as presented in [9], [14], is to approximate the optimal full state controller (6) by a linear combination of measurements as follows

$$u(t) = -\sum_{i=1}^{n_s} g_i(t)y_i(t), \tag{9}$$

where $y_i(t)$, $i = 1,\ldots,n_s$ denotes the n_s scalar measurements and $g_i(t)$ are their corresponding time-varying gains. In (9), it is assumed that there are n_s measurements given by

$$y(t) = \begin{bmatrix} y_1(t) & \cdots & y_{n_s}(t)\end{bmatrix}^T. \tag{10}$$

Summarizing, the controller (6) requires either full state information or the implementation of an estimator whereas the controller (9) requires n_s output measurements. Thus, to eliminate the computational cost, one must ensure that

$$\mathcal{K}(t)x(t) \approx \sum_{i=1}^{n_s} g_i(t)y_i(t), \tag{11}$$

is an appropriate sense. This approximation includes multi-level optimization since both the gains and the sensor locations associated with each output measurement $y_i(t)$ can be selected to minimize the difference $\mathcal{K}(t)x(t) - \sum_{i=1}^{n_s} g_i(t)y_i(t)$. In the event that the gain $\mathcal{K}(t)$ is time-varying, then the above can be optimized by moving the sensors associated with the output measurements $y_i(t)$.

Summarizing the earlier results in [9], [14], one assumes that the feedback operator $\mathcal{K}(t)$ admits a kernel representation and tries to simultaneously select the sensor locations and the gains to minimize the L_2 norm of this difference for all tests functions. In particular, when the sensor network is uniform, in the sense that the sensing devices are identical differing only on the location of their sensor, then the

approximation (11) becomes

$$\int_0^\ell k(t,\xi)x(t,\xi)\,\mathrm{d}\xi \approx \sum_{i=1}^{n_s} g_i(t)y_i(t), \tag{12}$$

for the 1D case, and

$$\iint_\Omega k(t,\xi,\psi)x(t,\xi,\psi)\,\mathrm{d}\xi\mathrm{d}\psi \approx \sum_{i=1}^{n_s} g_i(t)y_i(t), \tag{13}$$

for the 2D case. Continuing, using identical pointwise-in-space sensors, the output measurements are given by

$$y_i(t) = \int_0^\ell \delta(\xi-\xi_i(t))x(t,\xi)\,\mathrm{d}\xi,$$

for the 1D case, or for the 2D case by

$$y_i(t) = \iint_\Omega \delta(\xi-\xi_i(t))\delta(\psi-\psi_i(t))x(t,\xi,\psi)\,\mathrm{d}\xi\,\mathrm{d}\psi.$$

The approximations (12) or (13), in weak form, are given by

$$\min_{\phi\in\mathcal{V}}\left|\int_\Omega\left(k(t,\boldsymbol{\xi})-\sum_{i=1}^{n_s} g_i(t)\delta(\boldsymbol{\xi}-\boldsymbol{\xi}_i(t))\right)\phi(\boldsymbol{\xi})\,\mathrm{d}\boldsymbol{\xi}\right|, \tag{14}$$

where $\boldsymbol{\xi}=\xi\in(0,\ell)$ in 1D and $\boldsymbol{\xi}=(\xi,\psi)$ in 2D.

The idea presented in [9], [14], is to partition the kernel $k(t,\boldsymbol{\xi})$ in each time t in such a way that each partition carries the same level of control "authority". A pointwise sensor is placed in each partition for each time t and when the partitions become time-varying due to the time variation of $k(t,\boldsymbol{\xi})$, then the sensors within partition are also rendered time varying. This time-variation provides the spatial repositioning of the sensors within Ω. The second part of the optimization (14) is to find the time-varying gains g_i.

In parallel to the approximation (11) which may lead to mobile sensors, the actuator also moves and thus renders the feedback operator time varying. As summarized in [1], the application of an integrated optimal control and actuator guidance results in a computationally intensive control solution since it requires the backward-in-time integration of both a Riccati equation (8) and the actuator guidance. To reduce the control complexity, a suboptimal full-state feedback controller was proposed wherein the finite horizon cost (7) was substituted by an infinite horizon cost with the lower time switched at the beginning of a time-interval. This substitution resulted in a suboptimal controller but improved the real-time implementability since it required the solution to algebraic Riccati equations. The index (7) is now

$$J(t_i,x(t_i)) = \int_{t_i}^\infty \langle x(\tau),Qx(\tau)\rangle_{\mathcal{X}} + u^T(\tau)R^{-1}u(\tau)\,\mathrm{d}\tau \tag{15}$$

where the lower limit t_i is changed every Δt time units and replaced by $t_i \to t_i+\Delta t$. At the beginning of a new interval $[t_i,t_i+\Delta t)$, a new actuator location is selected by minimizing the optimal cost over the set of admissible actuator locations. In the earlier works, the set of admissible locations consisted of all locations that rendered the associated pairs $(\mathcal{A},\mathcal{B})$ approximately controllable. Incorporating realistic constraints resulting from the inclusion of vehicle motion, the set of admissible actuator locations was further restricted to the set of actuator locations that render the pair $(\mathcal{A},\mathcal{B})$ approximately controllable *and* ensure that the locations can be reached by the mobile platform within the Δt time units.

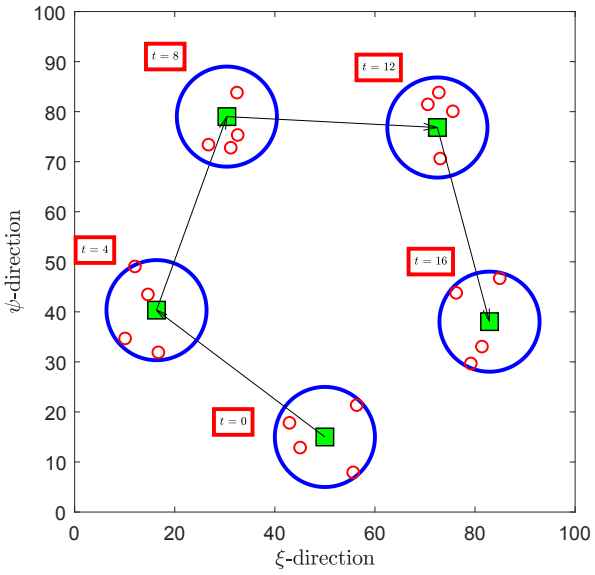

Fig. 1. Depiction of a mobile actuator (□) with its mobile sensors (○) orbiting its current position in the spatial domain at different time instances. Sensors are contained within a proximity region (circle) of the actuator.

The decomposition of the spatial domain Ω using kernel partitioning is summarized in the next section. The actuator selection at the beginning of a new interval $[t_i,t_i+\Delta t)$ will then be presented in Section IV.

III. Spatial Domain Decomposition via Feedback Kernel Partitioning

The feedback kernel associated the feedback operator $\mathcal{K}$ in (6) is desired to be decomposed according to (14). The basic idea is to divide Ω into n_s regions that have the same level of control "authority". This is interpreted as having the same area under the feedback kernel and this is determined by dividing the total area of the kernel $k(\xi)$ by n_s. For the 2D case, this is interpreted as evaluating the volume of the kernel $k(\xi,\psi)$ over Ω and dividing by n_s, [9].

The approach presented in [14] is summarized here and demonstrated for the 1D case. The spatial domain $\Omega=[0,\ell]=[0,1]$ is partitioned into n_s cells, each of which has the same area under the kernel and is equal to the total area A divided by n_s. Each cell in Ω is denoted by I_i, $i=1,\ldots,n_s$ with the property $I_i\cup I_j=\emptyset$ and $\bigcup_{i=1}^{n_s}\bar{I}_i=\bar{\Omega}$ and found via

$$\int_{I_i} k(\xi)\,\mathrm{d}\xi = \int_\Omega k(\xi)\,\mathrm{d}\xi/n_s = (A/n_s),\ i=1,\ldots,n_s.$$

Once the cells are found, one then places a single sensor ξ_s in each cell I_i. One way to achieve this is to place a sensor ξ_s in the cell I_i with the property that it further divides the cell $I_i=I_i^L\cup I_i^R$ into two equiareal subcells with respect to the kernel. In each subcell, one has

$$\int_{I_i^L} k(\xi)\,\mathrm{d}\xi = \int_{I_i^R} k(\xi)\,\mathrm{d}\xi = \frac{1}{2}\int_{I_i} k(\xi)\,\mathrm{d}\xi,\ i=1,\ldots,n_s.$$

Following [14], there is a very simple graphical method to compute the sensor locations ξ_i, $i=1,\ldots,n_s$ for the 1D case. For the 2D case, which produces level sets thereby suggesting multiple choices for sensor locations has been

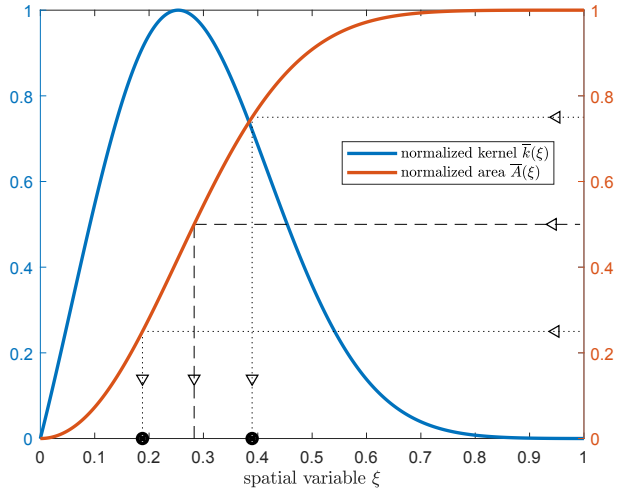

Fig. 2. Normalized kernel $\overline{k}(\xi)$ and its normalized areal function $\overline{A}(\xi)$. Domain $\Omega=[0,1]$ is partitioned into $n_s=2$ equiareal cells I_i with $\int_{I_i}k(\xi)\,\mathrm{d}\xi=\frac{1}{n_s}\int_0^1 k(\xi)\,\mathrm{d}\xi$. Sensor coordinates are found as the abscissae points on the normalized areal function $\overline{A}(\xi)$ having ordinates $0.25, 0.75$.

presented in [9]. Given a feedback kernel $k(\xi)$ associated with a feedback operator $\mathcal{K}$, define the normalized kernel and the associated normalized area function via

$$\overline{k}(\xi)=\frac{k(\xi)}{\max_{\xi\in\Omega}k(\xi)},\quad \overline{A}(\xi)=\frac{A(\xi)}{A(\ell)},\ A(\xi)=\int_0^{\xi}k(\xi)\,\mathrm{d}\xi.$$

From the above, it is easily observed that $\overline{A}(\ell)=1$ and that $\overline{A}(\xi)$ represents the fraction of the kernel area up to the spatial point ξ. All is left now is to plot the normalized area function $\overline{A}(\xi)$ and identify the ordinate points i/n_s, $i=1,\ldots,n_s$. The abscissae points corresponding to these ordinate points immediately identify the cells I_i. We identify the sensor locations ξ_i with the property

$$\xi_i:\int_0^{\xi_i}k(\xi)\,\mathrm{d}\xi=(2i-1))A/(2n_s),\quad i=1,\ldots,n_s.$$

Graphically, one identifies the ordinates $(2i-1)/(2n_s)$ on the $\overline{A}(\xi)$ graph and the abscissae reveal the sensor locations!

As an example, assume that $k(\xi)=\sin(\pi\xi)e^{-10(\xi-0.1)^2}$, $\xi\in[0,1]$. Figure 2 depicts the normalized kernel and the associated normalized areal function. For $n_s=2$, the domain is decomposed into $I_1=[0,0.283]$ and $I_2=[0.283,1]$ with the sensors placed at $\xi_1=0.188, \xi_2=0.389$.

Once the graphical method is applied to obtain the sensor locations in the approximation (14), one must calculate the feedback gains g_i. In the 1D case with Dirichlet boundary conditions, the space $\mathcal{V}=H_0^1(\Omega)$ and the optimization (14) is performed over all test functions $\phi\in H_0^1(\Omega)$. Assume that the feedback kernel has an expansion of the form $k(\xi)=\sum_{j=1}^N k_j\phi_j(\xi)$, $\forall\phi_j\in H_0^1(0,1)$. Applying this in (14) with the state $x(t,\xi)$ replaced by the test functions $\phi_k(\xi)$ one has

$$\min_{\phi\in\mathcal{V}}\left|\int_\Omega\left(\sum_{j=1}^N k_j\phi_j(\xi)-\sum_{i=1}^{n_s}g_i(t)\delta(\xi-\xi_i(t))\right)\phi_k(\xi)\,\mathrm{d}\xi\right|,$$

which when evaluated for all test functions $\phi_k(\xi)$ obtains the least-squares solution $M\kappa=\Phi(\xi_s)G$, where the $N\times N$ matrix M denotes the mass matrix given by $[M]_{jk}=\int_0^1\phi_j(\xi)\phi_k(\xi)\,\mathrm{d}\xi$, $j,k=1,\ldots,N$, and the vector of the kernel coefficients and of the static gains are

$$G=\begin{bmatrix} g_1 & \ldots & g_{n_s}\end{bmatrix}^T,\quad \kappa=\begin{bmatrix} k_1 & \ldots & k_N\end{bmatrix}^T.$$

The $N\times n_s$ regressor matrix $\Phi(\xi_s)$ is given by

$$\Phi(\boldsymbol{\xi}_s)=\begin{bmatrix}\phi_1(\xi_1) & \ldots & \phi_1(\xi_{n_s})\\ \vdots & \ddots & \vdots\\ \phi_N(\xi_1) & \ldots & \phi_N(\xi_{n_s})\end{bmatrix}.$$

By minimizing the $L^2(\mathbb{R}^N)$ norm of the error in $M\kappa=\Phi(\xi_s)\Gamma$, the least squares solution produces

$$G=\left(\Phi^T(\boldsymbol{\xi}_s)\Phi(\boldsymbol{\xi}_s)\right)^{-1}\Phi^T(\boldsymbol{\xi}_s)(M\kappa).$$

For the particular example, the corresponding gain is $G=\begin{bmatrix}0.50 & 0.38\end{bmatrix}$, thus approximating the full state control signal by the weighted sum of two pointwise state evaluations

$$\int_0^1\sin(\pi\xi)e^{-10(\xi-0.1)^2}x(t,\xi)\mathrm{d}\xi\approx$$
$$0.50x(t,0.188)+0.38x(t,0.389)=0.50y_1(t)+0.38y_2(t).$$

IV. Main Results

Having defined the approximation of (6) by a weighted sum of pointwise measurements in (11) enabled by the optimization (14), we now proceed with the main result. Combining the earlier result [1] on the use of time-varying reachability sets to account for vehicle motion constraints in selecting actuator locations, we extend the subsequent result in [2] to the employment of *not a single* collocated sensor, *but* of a network of sensors hovering the mobile actuator, as depicted in Figure 1. In this case, the vicinity region that the sensors are positioned with respect to the current actuator position is taken to coincide with the reachability region associated with the current actuator position.

Using the cost-to-to at the beginning of a new time interval $[t_k,t_k+\Delta t)$, one minimizes the cost

$$J(x(t_k),t_k)=\int_{t_k}^{\infty}\langle x(\tau),Qx(\tau)\rangle+Ru^2(\tau)\,\mathrm{d}\tau. \tag{16}$$

To select an actuator to be active over an interval $[t_k,t_k+\Delta t)$, one parameterizes the input operator $\mathcal{B}$ by the admissible actuator locations $\chi_a=(\xi_a,\psi_a)$. The set of admissible locations Θ_a consists of all the locations in Ω that render the location-parameterized pairs $(\mathcal{A},\mathcal{B}(\chi_a))$ approximately controllable. The location-parameterized input operator takes the form

$$\langle\mathcal{B}(\chi_a)u(t),\phi\rangle=\int_\Omega b(t,\xi,\psi;\xi_a,\psi_a)\phi(\xi,\psi)\,\mathrm{d}\xi\mathrm{d}\psi u(t). \tag{17}$$

The simultaneous actuator location and feedback operator gain can be obtained via

$$\begin{aligned}\chi_a^{opt,k}&=\arg\min_{\chi_a\in\Theta_a}\langle x(t_k),\mathcal{P}(\chi_a)x(t_k)\rangle,\\ \mathcal{K}^{opt,t_k}&=R^{-1}\mathcal{B}^*(\chi_a^{opt,k})\mathcal{P}(\chi_a^{opt,k}),\end{aligned} \tag{18}$$

where $\mathcal{P}(\chi_a)$ solves the location-parameterized ARE

$$\begin{aligned}0&=\langle\mathcal{A}\phi_1,\mathcal{P}(\chi_a)\phi_2\rangle+\langle\mathcal{P}(\chi_a)\phi_1,\mathcal{A}\phi_2\rangle\\ &-\langle\mathcal{P}(\chi_a)\mathcal{B}(\chi_a)R^{-1}\mathcal{B}^*(\chi_a)\mathcal{P}(\chi_a)\phi_1,\phi_2\rangle+\langle Q\phi_1,\phi_2\rangle,\end{aligned} \tag{19}$$

for all $\phi_1, \phi_2 \in V$.

When the vehicle carrying the actuating devices is taken into account, then one cannot use the entire spatial domain Ω for the next actuator location since it is almost impossible for a mobile platform to traverse large distances over finite time intervals. The search for an actuator in the time interval $[t_k, t_k + \Delta t)$ must be constrained to the region that can be reached within a finite amount of time. We use the following kinematic equations to represent the motion of a mobile platform within a 2D domain

$$\begin{aligned} \dot{\xi}_a(t) = v(t)\cos(\theta_a(t)),\ \dot{\psi}_a(t) = v(t)\sin(\theta_a(t)), \\ \dot{\theta}_a(t) = \omega_a(t), \end{aligned} \tag{20}$$

with the speed $v(t)$ and turning rate $\omega_a(t)$ the control signals.

To quantify the region where the search for the next actuator location will take place, it is assumed that an actuator will reside in a given position for Δt time units and will move to its new position at the beginning of a new time interval. Assuming uniform time intervals

$$t_k = t_0 + k\Delta t, \qquad k = 1, 2, \ldots, (T - t_0)/\Delta t - 1,$$

we require that the platform carrying the actuator will move to its new desired position within a travel time t_{travel} that is significantly less than the residence time Δt.

In other words, at the beginning of a new time interval $[t_k, t_k + \Delta t)$ of duration Δt, the mobile platform must move to a new position within the travel time t_{travel}. If the actuator optimization predicts a new position that is far away from the current position χ_a^{opt,t_k}, the platform will not be able to move to the new position. Thus, the search for the next actuator position, must be restricted to a subset of Θ_{ad} which consists of all the candidate locations that render the pairs $(\mathcal{A}, \mathcal{B}(\chi_a))$ approximately controllable *and* can be reached from the current position within t_{travel}. Further assuming a constant speed for simplicity, the set of points that can be reached from the current position $(\xi(t_k), \psi(t_k))$ within the travel time t_{travel} is given by

$$\begin{aligned} \xi(t) &= \xi(t_k) + (vt_{travel})\cos(\theta(t)), \\ \psi(t) &= \psi(t_k) + (vt_{travel})\sin(\theta(t)). \end{aligned} \tag{21}$$

Thus, the time-varying reachability sets that are used to search for the candidate actuator locations at the beginning of a new time interval $[t_k, t_k + \Delta t)$ are defined via

$$\begin{aligned} \mathcal{R}_1(t_k) = \Theta_a \cap \Big\{ (\theta, \psi, \theta) : (\xi, \psi) \text{ satisfy (21)} \\ \text{for } -\pi \le \theta(t) \le \pi \Big\}, \end{aligned} \tag{22}$$

As presented in [2], there are two additional time-varying reachability sets that result by incorporating motion constraints; for example, when the mobile platform has to obey angular constraints $\theta(t) \in [\theta_a(t_k) - \Delta\theta, \theta_a(t_k + \Delta\theta]$ the associated time-varying reachability set is given by

$$\begin{aligned} \mathcal{R}_2(t_k) = \Theta_a \cap \Big\{ (\theta, \psi, \theta) : (\xi, \psi) \text{ satisfy (21)} \\ \text{for } \theta_a(t_k) - \Delta\theta \le \theta(t) \le \theta_a(t_k) + \Delta\theta \Big\}. \end{aligned}$$

A third reachability set imposes both angular and angular rate constraints and is described in [1].

One of the problems that arise is that the optimization (18) cannot be realized since the full state is not available. The other problem is that the sensors, as can be predicted by the method in Section III, must be constrained also within the time-varying residual set. The reason is that for a given actuator location, the resulting optimal controller gain using the approximation (11) may place the sensors far away from the current actuator location. To address this, and essentially realize the schematic in Figure 1, one must also restrict the sensors to the vicinity of the current actuator location. This vicinity is taken for simplicity to be the time-varying reachability set associated with the actuator location.

Thus, for each $t \in [t_k, t_k + \Delta t)$, the actuator location is selected via (18), but with the search restricted to the time-varying reachability set (22) and given here by

$$\begin{aligned} \chi_a^{opt,t_k} &= \arg\min_{\chi_a \in \mathcal{R}_1(t_k)} \langle x(t_k), \mathcal{P}(\chi_a) x(t_k) \rangle, \\ \mathcal{K}^{opt,t_k} &= R^{-1}\mathcal{B}^*(\chi_a^{opt,k})\mathcal{P}(\chi_a^{opt,k}). \end{aligned} \tag{23}$$

Once the actuator χ_a^{opt,t_k} and its associated feedback gain $\mathcal{K}^{opt,t_k}$ are selected, one then locates the sensors in the vicinity of the actuator using

$$\min_{\phi \in \mathcal{V}} \Big| \int_{\mathcal{R}_1(t_k)} \left(k^{opt,t_k}(\boldsymbol{\xi}) - \sum_{i=1}^{n_s} g_i^{t_k} \delta(\boldsymbol{\xi} - \boldsymbol{\xi}_i^{t_k}) \right) \phi(\boldsymbol{\xi})\, d\boldsymbol{\xi} \Big|, \tag{24}$$

where $k^{opt,t_k}(\boldsymbol{\xi})$ is the kernel associated with the feedback operator $\mathcal{K}^{opt,t_k}$ and $\boldsymbol{\xi}_i^{t_k}$, $i = 1, \ldots, n_s$ are the sensor locations within $\mathcal{R}_1(t_k)$ that optimize (24) with $g_i^{t_k}$ their static gains.

One way to interpret the above is to view the mobile sensors as following the mobile actuator and repositioning themselves around the current actuator location within the reachability set $\mathcal{R}_1(t_k)$. The orientation and distribution of the sensors in the vicinity of the actuator may be different for different times, but at each time all the sensors are within the current reachability set $\mathcal{R}_1(t_k)$.

To address the fact that the state $x(t_k)$ in (18) or (23) is not available, we modify the approach considered in [2]. In a time interval $[t_k, t_k + \Delta t)$, one computes the optimal feedback gain associated with each candidate actuator location in $\mathcal{R}_1(t_k)$ and find the sensors associated with the decomposition of that feedback gain. The to select the candidate actuator with the associated sensors and static gains, consider the resulting closed-loop system

$$\dot{x}(t) = (\mathcal{A} - \mathcal{B}(\chi_a)G(\chi_a)\mathcal{C}(\chi_a))x(t), \tag{25}$$

and select the energy-to-go given by

$$E(t_k, \chi_a) = \int_{t_k}^{\infty} \langle x(\tau), \mathcal{M}x(\tau) \rangle\, d\tau, \tag{26}$$

whose value is given by $E(t_k, \chi_a) = \text{trace}\ (\Sigma(\chi_a))$ where $\Sigma(\chi_a)$ solves the location-parameterized operator equation

$$\begin{aligned} (\mathcal{A} - \mathcal{B}(\chi_a)G(\chi_a)\mathcal{C}(\chi_a))^* \Sigma(\chi_a) \\ + \Sigma(\chi_a)(\mathcal{A} - \mathcal{B}(\chi_a)G(\chi_a)\mathcal{C}(\chi_a)) = -\mathcal{M}. \end{aligned} \tag{27}$$

An alternate decision for the actuator selection with its associated sensors is to use the sensor measurements associated with each actuator location and compare the norm of the

output signal as an approximation and substitute for the state norm. This of course has to run by one time-step behind the selection of the actuator location.

Algorithm 1 summarizes the proposed actuator selection using time-varying reachability sets and the associated sensors and feedback gains.

Algorithm 1 Actuator-sensor guidance in $[t_k, t_{k+1})$

1: **initialize:** Determine the set of admissible actuator locations Θ_{ad} that render the location-parameterized operators $(\mathcal{A}, \mathcal{B}(\chi_a))$ approximately controllable. Divide the interval of interest $[t_0, T]$ into n uniform subintervals $[t_k, t_{k+1}]$ with $t_k = t_0 + k\Delta t$ and $\Delta t = (T - t_0)/n$. The Δt is selected using hardware and processor requirements.
2: **iterate:** $k = 0$
3: **loop**
4: Define the reachability set $\mathcal{R}_1(t_k)$ using (22)
5: For each $\chi_a \in \mathcal{R}_1(t_k)$, compute the gains $\mathcal{K}(\chi_a)$ and the associated kernels $k(\chi_a)$ using the ARE (19).
6: Using (24), calculate the candidate sensor locations and their static gains for each $\chi_a \in \mathcal{R}_1(t_k)$.
7: Minimize the actuator location-parameterized energy-to-go (26) over all $\chi_a \in \mathcal{R}_1(t_k)$
8: Select the actuator location for $[t_k, t_{k+1})$ using

$$\chi_a^{opt,t_k} = \arg \min_{\chi_a \in \mathcal{R}(t_k)} \operatorname{trace}(\Sigma(\chi_a))$$

where $\Sigma(\chi_a)$ solves the Lyapunov equation (27)
9: For $t \in [t_k, t_{k+1})$, use (21) move to actuator location χ_a^{opt,t_k} within the appropriate reachability set $\mathcal{R}_1(t_k)$ and implement the static output feedback controller

$$u(t) = -G(\chi_a^{opt,t_k})C^*(\chi_a^{opt,t_k})x(t) = -G(\chi_a^{opt,t_k})y^{opt,t_k}(t$$

10: Propagate the relevant PDE (2) or (4) in $[t_k, t_{k+1})$
11: **if** $k \leq n-2$ **then**
12: $k \leftarrow k+1$
13: **goto** 2
14: **else**
15: terminate
16: **end if**
17: **end loop**

V. Numerical Examples

PDE in 1D: Equation (2) is considered with $\alpha = 10$, $\beta = 0.05$ and $\gamma = -3 \times 10^{-4}$. The spatial domain is taken as $\Omega = [0, \ell] = [0, 100]$m. A single actuator can move with $v = 25$m/s and can reside in a given position for $\Delta t = 4$s. Using a travel time $t_{travel} = 0.4$s, the reachability radius is $\mathcal{R} = 10$m, meaning that at a given actuator location $\xi_a^{t_k}$, the reachability set is $\mathcal{R}_1(t_k) = \{\xi : \xi_a^{t_k} - \mathcal{R} \leq \xi \leq \xi_a^{t_k} + \mathcal{R}\}$. The LQR parameters in (19) were chosen as $Q = I, R = 10^{-2}$.

A Galerkin-based finite dimensional approximation was used to approximate (2) with 200 linear elements and the resulting set of differential equations was simulated with the ODE solver `ode45` in Matlab®.

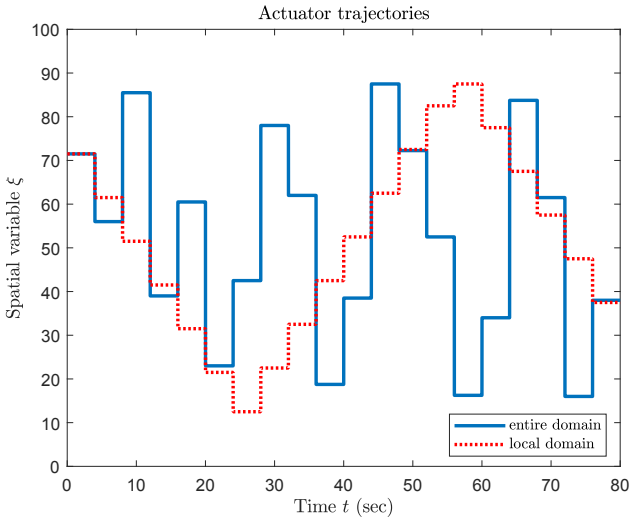

Fig. 3. Actuator trajectory using the decomposition (14) over the entire Ω and the decomposition (24) over the time-varying reachability sets $\mathcal{R}(t_k)$.

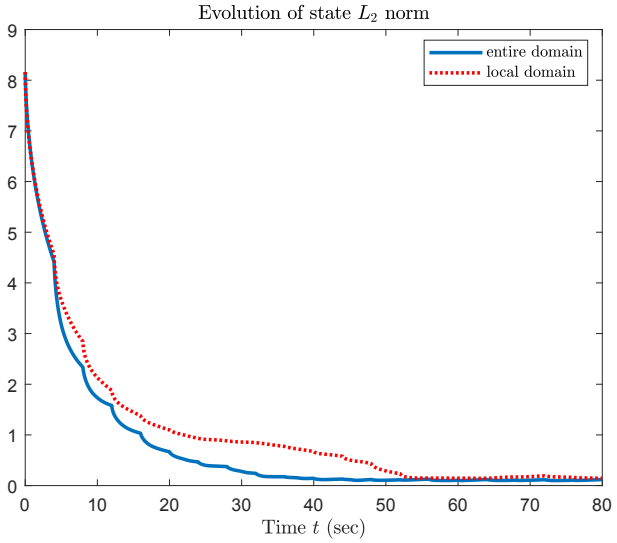

Fig. 4. Evolution of L_2 state norm.

Figure 3 depicts the actuator trajectories when the proposed kernel decomposition method with the $n_s = 7$ sensors are also constrained to lie within the reachability set. For comparison, the decomposition method with the sensors allowed to be positioned within Ω is also included. For the former, the decomposition (24) is used, whereas for the latter, the decomposition (14) is used. It is observed that completely different actuator trajectories are predicted.

To examine the performance of the decompositions (14) and (24), the L_2 norm of the closed loop state is presented in Figure 4. It is observed that when the sensors approximating the kernel are allowed to be located within Ω, via (24), the performance of the closed-loop system is slightly better as expected. However, the benefit in using the time-varying reachability set to perform the kernel decomposition (24) lies with the realistic situation of the mobile sensors lying in the vicinity of the current position of the actuating device.

PDE in 2D: The PDE in (4) was considered with $\alpha =$

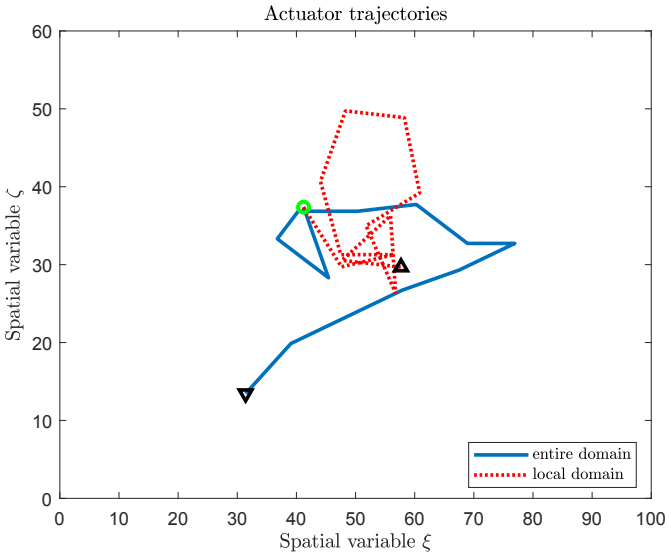

Fig. 5. Actuator trajectory using the kernel decomposition (14) over the entire domain and the decomposition (24) over the time-varying reachability sets $\mathcal{R}(t_k)$.

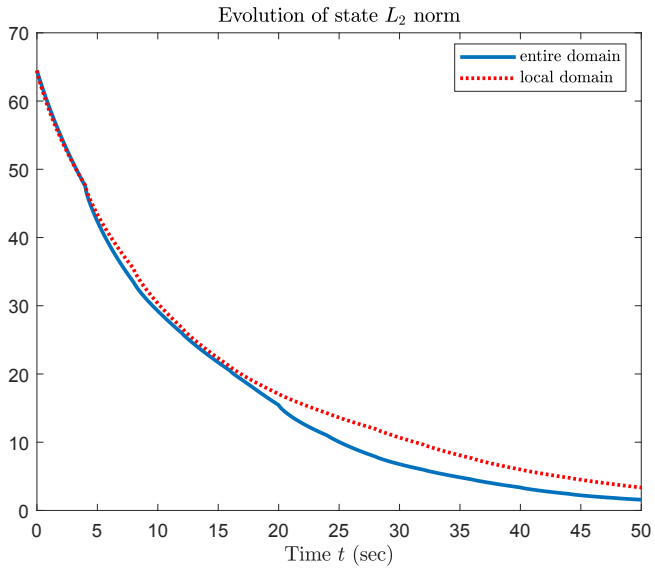

Fig. 6. Evolution of L_2 state norm.

$10, \beta = 1.5 \times 10^{-4}, \gamma = -3 \times 10^{-4}$ over the spatial domain $\Omega = [0, L_\xi] \cup [0, L_\psi] = [0, 100] \cup [0, 60]$m. The mobile platform carrying the actuator had a speed of $v = 25$/s and can take $t_{travel} = 0.4$s to travel to a new position, thereby resulting in a reachability radius $\mathcal{R} = 10$m. For a given actuator position $\chi_a^{t_k}$, the resulting reachability set (22) is given by a circle of radius $\mathcal{R}$ centered at $\chi_a^{t_k}$. The LQR parameters in (19) were similarly taken as $Q = 10I$ and $R = 10^{-2}$.

The PDE (4) was approximated by a Galerkin scheme using $n_x = 41$ and $n_y = 26$ elements over $[0, L_\xi]$ and $[0, L_\psi]$.

The trajectories using the reachability set for kernel decomposition (24) and using the entire domain for kernel decomposition (14) are presented in Figure 5. As in the 1D case, the trajectories are very different for the decomposition using the entire domain and the time-varying reachability set.

VI. Conclusions

A method for decomposing a feedback kernel based on a computational geometry method was proposed for a class of PDEs. The state feedback controller was replaced by a weighted sum of sensor measurements in order to reduce controller complexity and minimize computational load. At the beginning of a new time interval, a mobile actuator is repositioned to a new location using an LQR actuator optimization restricted to a time-varying reachability set that took into account vehicle dynamics. Ensuring that the sensors used to approximate the kernel decomposition, a further restriction was imposed which force the mobile sensors to remain in the vicinity of the current position of the actuator.

The feedback kernel decomposition and the constrained sensor positioning within the time-varying reachability set of the mobile actuator constituted the novelty of the reported results.

References

[1] M. A. Demetriou, "Controlling PDEs with mobile actuators constrained over time-varying reachability sets," in *Proc. of the 59th IEEE Conference on Decision and Control*, 2020, pp. 4411–4416.

[2] ——, "Controlling 2D PDEs using mobile collocated actuators-sensors and their simultaneous guidance constrained over path-dependent reachability regions," in *Proc. of the American Control Conference*, 2021, pp. 1491–1496.

[3] J. A. Burns and B. B. King, "Optimal sensor location for robust control of distributed parameter systems," in *Proceedings of the 33rd IEEE Conference on Decision and Control*, vol. 4, Dec 1994, pp. 3967–3972.

[4] J. A. Burns and D. Rubio, "A distributed parameter control approach to sensor location for optimal feedback control of thermal processes," in *Proceedings of the 36th IEEE Conference on Decision and Control*, vol. 3, 10-12 Dec 1997, pp. 2243–2247.

[5] A. L. Faulds and B. B. King, "Sensor location in feedback control of partial differential equation systems," in *Proc. of the IEEE Int'l Conference on Control Applications*, 25-27 Sep 2000, pp. 536–541.

[6] I. Akhtar, J. Borggaard, J. A. Burns, H. Imtiaz, and L. Zietsman, "Using functional gains for effective sensor location in flow control: a reduced-order modelling approach," *J. of Fluid Mechanics*, vol. 781, pp. 622–656, 10 2015.

[7] M. A. Demetriou, "Sensor selection and static output feedback of parabolic PDEs via state feedback kernel partitioning using modification of voronoi tessellations," in *Proc. of the American Control Conference*, May 2017, pp. 2497–2503.

[8] M. A. Demetriou, "Using modified centroidal voronoi tessellations in kernel partitioning for optimal actuator and sensor selection of parabolic PDEs with static output feedback," in *Proc. of the IEEE 56th Annual Conference on Decision and Control*, 2017, pp. 3119–3124.

[9] M. A. Demetriou and W. Hu, "Feedback kernel approximations and sensor selection for controlled 2D parabolic PDEs using computational geometry methods," in *Proc. of the IEEE 58th Conference on Decision and Control*, 2019, pp. 2144–2150.

[10] R. E. Showalter, *Hilbert Space Methods for Partial Differential Equations*. London: Pitman, 1977.

[11] J. A. Burns, E. M. Cliff, and C. Rautenberg, "A distributed parameter control approach to optimal filtering and smoothing with mobile sensor networks," in *Proc. of the 17th Mediterranean Conference on Control and Automation*, Thessaloniki, Greece, June 24-26 2009.

[12] ——, "Optimal sensor design for estimation and optimization of PDE systems," in *Proc. of the American Control Conference*, Baltimore, MD, June 30- July 2 2010.

[13] J. A. Burns and C. N. Rautenberg, "The infinite-dimensional optimal filtering problem with mobile and stationary sensor networks," *Numer. Funct. Anal. Optim.*, vol. 36, no. 2, pp. 181–224, 2015.

[14] M. A. Demetriou, "Employing mobile sensor density to approximate state feedback kernels in static output feedback control of PDEs," in *Proc. of the American Control Conference*, 2021, pp. 2775–2781.